Journal of Anatomy

J. Anat. (2016) **229**, pp326–333 doi: 10.1111/joa.12475

METHOD

A method to quantify and visualize femoral head intraosseous arteries by micro-CT

Xing Qiu,[1,2] Xiaotian Shi,[3] Jun Ouyang,[1] Dachuan Xu[1] and Dewei Zhao[1,2]

[1]*Department of Anatomy, Guangdong Provincial Key Laboratory of Medical Biomechanics, School of Basic Medicine Science, Southern Medical University, Guangzhou, Guangdong, China*
[2]*Department of Orthopedics, Affiliated Zhongshan Hospital of Dalian University, Dalian, Liaoning, China*
[3]*Department of Anatomy, Hainan Medical College, Haikou, Hainan, China*

Abstract

We describe a technique for perfusing a barium sulphate suspension into the intraosseous artery. Following the perfusion of abarium sulphate suspension into 14 fresh lower limbs of Chinese cadavers, micro-CT scanning was applied to digitize, quantify and visualize the intraosseous arteries in the human femoral heads. Then, the femoral heads were removed and subjected to micro-CT scanning. The data were imported into the AMIRA and MIMICS programs to reconstruct and quantify the intraosseous arteries. The femoral head intraosseous artery lengths, areas, volumes, and femoral head bone volumes were quantified. The artery densities and artery ratios were calculated and analysed with independent-samples *t*-tests. The intraosseous vasculature volume renderings were displayed as screenshots and videos made with AMIRA. Many intraosseous artery study technologies were compared. The barium sulphate suspension was milky white in colour. The perfusion of the barium sulphate suspension followed by micro-CT scanning provided a good representation of the intraosseous artery. The femoral head intraosseous artery lengths, areas and volumes, and the femoral head bone volumes were displayed as the $\bar{X} \pm S$. No differences were observed between the left and right femoral head intraosseous arteries in terms of the artery densities or artery ratios. The volume renderings and 3-D orthogonal projections displayed the overall distributions of the intraosseous arteries. The videos clearly demonstrated the entry sites of the nutrition-carrying arteries, their courses and branches, and the intraosseous arterial anastomoses. Our technique is the simplest and least time-consuming method of producing accurate vascular three-dimensional reconstructions. The perfusion of a barium sulphate suspension into intraosseous arteries combined with micro-CT scanning can deliver high-resolution 3-D digitized data and images of intraosseous arteries. This technique does not require bone decalcification or bone dissection and thus significantly shortens the time required to quantify and display intraosseous arteries. This method provides a simple and rapid technique for quantifying and visualizing human intraosseous arteries.

Key words: artery; femoral head; intraosseous; micro-CT; vasculature.

Introduction

Femoral neck fractures occur frequently, and the complications of femoral head necrosis, delayed union and nonunion are well recognized. Femoral neck fracture healing is thought to be related to vascular anatomy. Studies of intraosseous arteries have traditionally been challenging due to the hard, calcified structure of bone. A variety of methods for investigating intraosseous arteries have been reported in the literature and typically involve bone clearance using the modified Spalteholz technique (Sheetz et al. 1995; Havet et al. 2008; Lamas et al. 2009; Koslowsky et al. 2011; McKeon et al. 2012; Papakonstantinou et al. 2012; Oppermann et al. 2014). However, the Spalteholz transparency technique is time-consuming and complex. Moreover, the three-dimensional (3-D) distribution of the intraosseous arteries of the femoral head is still not well known due to the limitations of traditional techniques (Sheetz et al. 1995; Havet et al. 2008; Lamas et al. 2009; Koslowsky et al. 2011; McKeon et al. 2012; Papakonstanti-

Correspondence
Dewei Zhao, No. 6 Jiefang Street, Dalian, Liaoning 116001, China.
T: + 86 411 62893509; E: zhaodewei2000@163.com

Accepted for publication *1 March 2016*
Article published online *14 April 2016*

nou et al. 2012; Oppermann et al. 2014). Recently, micro-computed tomography has been widely utilized to perform highly accurate quantifications of the three-dimensional vascular networks of tumours, coronary arteries and the entire brain vasculature (Lerman & Ritman, 1999; Lee et al. 2007; Langheinrich et al. 2010). The goal of this study was to describe a technique involving the perfusion of a barium sulphate suspension into an intraosseous artery combined with micro-CT scanning to digitize, quantify and visualize the human intraosseous artery of the femoral head.

Material and methods

Our Institutional Review Board granted institutional approval for this study and the procurement of lower limbs from the body donation programme associated with Southern Medical University. We used 14 Chinese fresh-frozen cadaveric fresh lower limbs (nine left legs and five right legs from one female and 13 males) for this study. The mean donor age at the time of death was 37.2 years (range 25–67). All donors were free from any previous hip pathologies and surgeries and had no known history of previous traumatic injuries or congenital abnormalities. Due to certain factors that currently remain beyond our control, i.e. vasospasms and post-mortem intravascular clotting, we injected more samples than we report here. We compared different techniques for the perfusion and display of the intraosseous artery vessels. Each technique involved injection, corrosion, and intraosseous artery display and recording (Fig. 4).

Contrast agent preparation and perfusion methods

The contrast agent used in this study was 30% barium sulphate in a 5% gelatine suspension. We prepared this agent by adding 100 g of gelatin (Cat. No. V900863, Sigma, 3050 Spruce Street, St. Louis, MO 63103, USA) to 2000 mL water in a beaker placed in a water bath at 80 °C to melt the gelatine. The water bath temperature was then decreased to 37 °C, and 600 g of barium sulphate was added to the gelation suspension (Blanc Fixe Micro, Sachtleben Chemie GmbH; mean grain size: 700 nm).

Perfusion of the contrast agent into the fresh specimens

In each lower limb, the femoral artery was exposed at the midpoint of the inguinal ligament. The technique used to visualize the intraosseous arteries of the femoral head was based on those previously described in investigations of human femoral head artery visualization with the use of any anti-coagulating buffers (Trueta & Harrison, 1953; Judet et al. 1955; Sevitt & Thompson, 1965). A customized catheter (φ = 3 mm) was sequentially inserted into the 14 femoral arteries and fastened by ligation. A rubber band was forcefully tied at the middle segment of the thigh. The lower limb was placed in a 37 °C water bath 2 h prior to the perfusion. A device that created and maintained a constant pressure (130–140 mm Hg) was used for at least 20 min to perfuse the suspension into the femoral artery. This process enabled high-resolution observation of the fine details of the artery distribution. After the perfusion, the hip was placed in a 0 °C water bath for 4 h to allow for the suspension to enter a gel state. Finally, we dissected the femoral heads for micro-CT scanning.

Micro-CT scanning, intraosseous artery 3-D reconstruction and quantification: image screenshots and video records

We fixed the femoral head on a scanning bed and scanned it under the same conditions using a micro-CT scanner (Table 1). The resolution was 24.37 μm.

The digitized femoral head data were imported into the Image Research Workplace (Siemens Medical Solutions, Inc., Illinois, USA) image analysis software program and exported as a file in the digital imaging and communications in medicine (DICOM) format. The data were then imported into amira 5.4.3, the intraosseous 3-D artery was reconstructed, and the femoral head intraosseous artery length was quantified. The data were imported into mimics 14.0, the intraosseous 3-D arteries were reconstructed, and the femoral head intraosseous artery area and volume and femoral head bone volume (using the same threshold for all samples) were quantified. The artery length density (artery length/bone volume), artery area density (artery area/bone volume), artery volume density (artery volume/bone volume), artery length/volume ratio and artery area/volume ratio were separately calculated.

The left and right femoral head intraosseous artery length densities, area densities, volume densities, artery length/volume ratios, and artery area/volume ratios were statistically analysed with independent-samples *t*-tests (SPSS 17.0, Inc., Chicago, IL, USA). The left and right femoral head intraosseous artery lengths, artery areas, artery volumes, and femoral head bone volumes are presented as $\bar{X} \pm S$.

The artery volume rendering and 3-D orthogonal projection view of the intraosseous vasculature are presented as screenshots and videos captured with amira.

Results

Contrast agent properties and enhancement effect

The barium sulphate suspension formed a gel within 2 h. The evenly distributed suspension was milky white, and the uniformly distributed grains were observed with a light microscope. The intraosseous arterial perfusion with

Table 1 Micro-CT scan parameter settings [Inveon Multimodality Scanner (Siemens, USA)].

CT scan		X-ray detector setup		X-ray tube setup		Field of view	
Start position (degrees)	0.00	Exposure time (ms)	200	Voltage (KV)	80	Trans-axial (mm)	49.92
Total rotation (degrees)	360.00	Effective pixel size (μm)	24.37	Current (μA)	500	Axial (mm)	49.92
Rotation steps (degrees)	360						
Estimated scan time (s)	451						

the barium sulphate suspension followed by micro-CT enabled the demonstration of the intraosseous arteries (Figs 1 and 2).

Volume-rendering and 3-D orthogonal projection of the intraosseous arteries of the femoral head

The distribution of the femoral head intraosseous arteries was demonstrated with the volume rendering and 3-D orthogonal projection techniques of the AMIRA software (Fig. 2). In the 3-D orthogonal projection images, the sites at which the nutritional arteries entered the bone, their diameters, the arterial trunk and its branches, and the intraosseous arterial anastomoses were all clearly demonstrated.

Digitization of the intraosseous artery of the femoral head in the DICOM format for quantification

The digitized data contained but were not limited to the following information: (i) the trabecular morphology and distribution; (ii) the intraosseous artery length, area, volume, and femoral head bone volume; (iii) the artery length density (artery length/bone volume), artery area density (artery area/bone volume) and artery volume density (artery volume/bone volume); (iv) the artery length/volume ratio and artery area/volume ratio (Table 2, Fig. 3); and (v) the intraosseous artery anastomoses and the branching patterns of the intraosseous artery.

Three-dimensional movies of the intraosseous arteries of the femoral head are presented as Supporting Information (Movies S1 and S2). The femoral head intraosseous artery length, artery area, artery volume and femoral head bone volume are presented as the $\bar{X} \pm S$ (Table 2, Fig. 3). No significant differences were found between the right and left femoral head intraosseous artery length densities, artery area densities, artery volume densities, artery length/volume ratios or artery area/volume ratios (Table 2, Fig. 3).

Discussion

To the best of our knowledge, this is the first report to quantify and visualize entire normal human femoral head intraosseous arteries using micro-CT. Currently, routine clinical CTs and MRIs cannot distinguish the intraosseous blood vessels. A variety of methods for investigating the intraosseous vasculature have been developed and reported in the literature, including micro-radiography, serial histological sectioning, and the intraosseous injection of epoxy resin, India ink or latex followed by bone clearing using a modified Spalteholz technique (Fig. 4) (Sheetz et al. 1995; Havet et al. 2008; Lamas et al. 2009; Koslowsky et al. 2011; McKeon et al. 2012; Papakonstantinou et al. 2012; Oppermann et al. 2014). However, these methods require bone decalcification, which makes it difficult to demonstrate the blood vessels in a single, whole 3-D structure and to quantify the intraosseous arteries. In contrast, the known arteries can be described in greater detail using our method. We investigated the previously undescribed parameters of artery length, area and volume, femoral head bone vol-

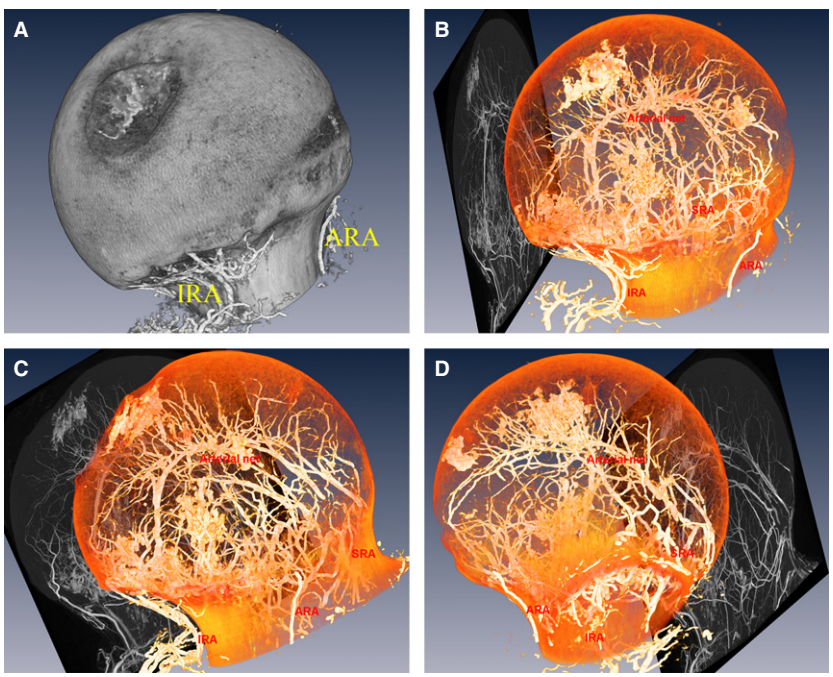

Fig. 1 Reconstruction of the left femoral head, orthogonal projection views of the arterial network and 3-D reconstruction of the intraosseous vascular of the left femoral head. The superior retinacular artery (SRA), the inferior retinacular artery (IRA) and the anterior retinacular artery (ARA) anastomoses within femoral head are shown. A 3-D reconstruction of the left femoral head andits arterial networks: medial-sagittal views of the left femoral head (A), medial-sagittal view of the left intraosseous arteries (B), front view (C), and lateral view (D).

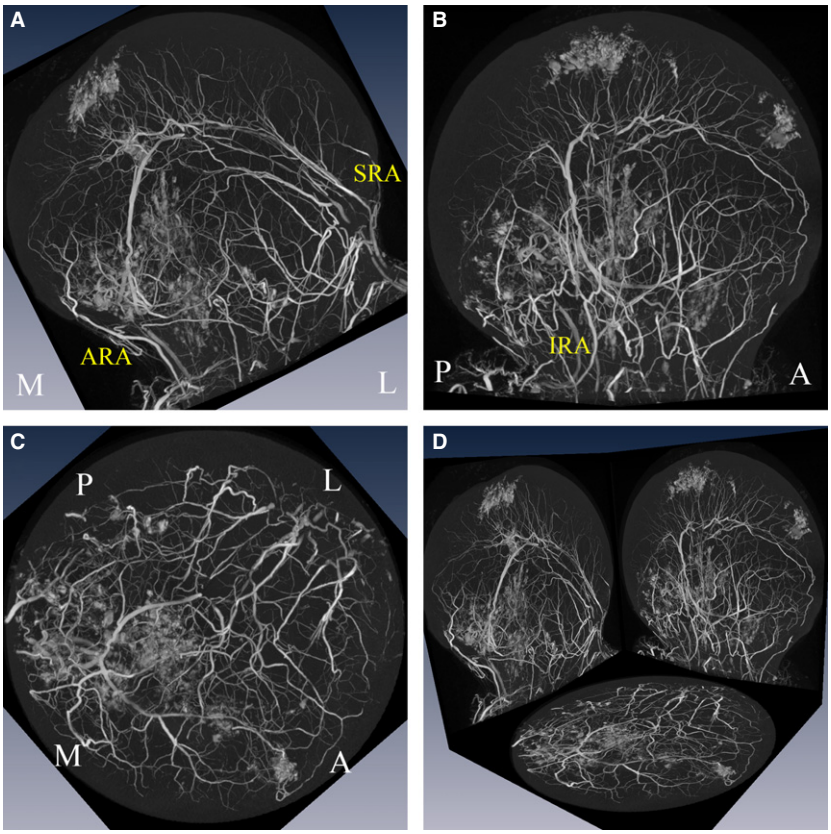

Fig. 2 Three-dimensional orthogonal projection views of the intraosseous arterial network of the left femoral head. Coronal view (A), medial-sagittal view (B), transverse view (C), and 3-D orthogonal projection (D) views of the left femoral head showing the anastomoses of the superior (SRA), inferior (IRA) and anterior (ARA) retinacular arteries. M, L, A and P corresponds to medial, lateral, anterior and posterior, respectively.

Table 2 Femoral head intraosseous artery length, area, volume, length density, area density, volume density, artery length/volume ratio, artery area/volume ratio and femoral head bone volume ($\bar{X} \pm S$).

Femoral head	Artery length (mm)	Artery area (mm^2)	Artery volume (mm^3)	Bone volume (mm^3)	Artery length density*	Artery area density*	Artery volume density*	Artery length/ volume*	Artery area/volume*
Left (n = 9)	4162 ± 2358 (n = 8)	3177 ± 1909	218.29 ± 130.92	27 807 ± 6649	0.1509 ± 0.0753 (n = 8)	0.1118 ± 0.0538	0.0076 ± 0.0037	19.72 ± 7.50 (n = 8)	14.68 ± 2.64
Right (n = 5)	3194 ± 988	2502 ± 851	180.13 ± 43.64	26 191 ± 3839	0.1226 ± 0.0381	0.0951 ± 0.0284	0.00681 ± 0.0008	18.04 ± 5.03	13.86 ± 3.25

Artery length density = artery length/bone volume; artery area density = artery area/bone volume; artery volume density = artery volume/bone volume.
*Independent-samples t-test analyses, $P < 0.05$. No significant differences were observed between the right and left femoral heads.

ume, artery length density, artery area density and artery volume density.

In the early stage of our study, we found that an epiphyseal arterial network is located above the epiphyseal scar/plate. The superior retinacular artery, the inferior retinacular artery, the anterior retinacular artery and the round ligament artery formed the arterial network. However, traditional reports of the femoral head artery distribution have not referred to these anatomical structures. Moreover, the traditional understanding of defects may have been limited by technical methods. The novel understanding of the distribution of the blood flow of the intraosseous arteries of the femoral head will provide evidence that will enable clinical improvements in femoral neck fracture internal fixation and the protection of the arteries. However, our sample size and thus our statistical power were low. Therefore, this content is not described here. This study discusses only the feasibility of this technique for quantifying and visualizing the intraosseous arteries of the femoral head using micro-CT.

Importance of knowledge about the intraosseous vasculature

It is important to visualize and quantify the intraosseous artery because the blood supply is essential to every cell. The use of this technique can aid the understanding of the mechanisms underlying bone necrosis, osteoporosis,

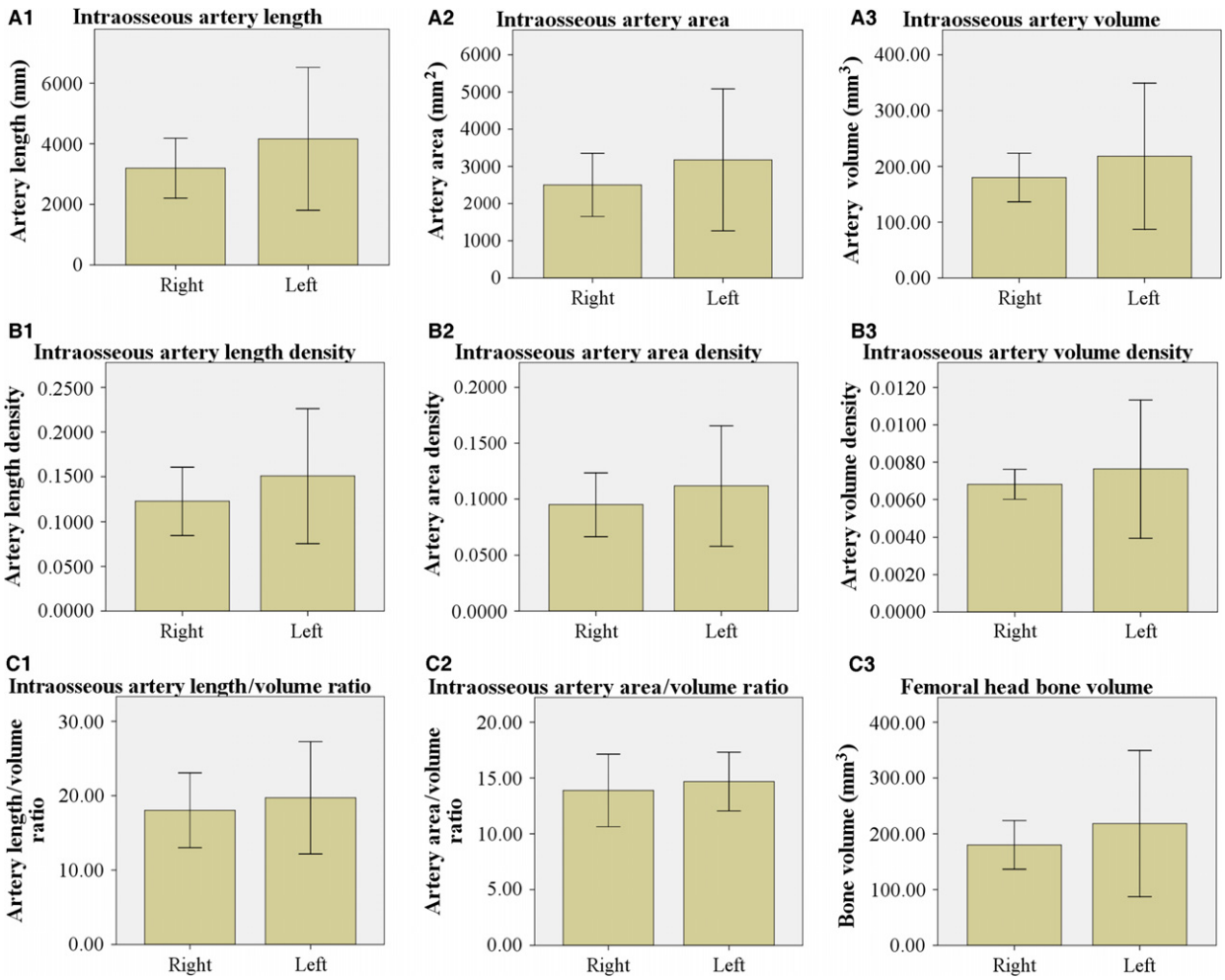

Fig. 3 Parameters of the femoral head intraosseous artery. Artery length (A1), area (A2), volume (A3), length density (B1), area density (B2), volume density (B3), artery length/volume ratio (C1), artery area/volume ratio (C2), femoral head bone volume (C3), and a statistical chart presented as the $\bar{X} \pm S$. Artery length density = artery length/bone volume, artery area density = artery area/bone volume, artery volume density = artery volume/bone volume. Independent-samples *t*-test analyses of the artery length density, area density, volume density, artery length/volume ratio, and artery area/volume ratio ($P < 0.05$). No significant differences were observed between the right and left femoral heads.

fracture healing, etc. Various diseases affect the blood supplies to intraosseous arteries. For example, conditions related to the femoral head, talus, scaphoid, cuneiform, clavicle, humeral head, radial head, distal humerus, distal radius and lunate have been reported, which indicates that these structures are vulnerable to vascular insult due to various causes (Meyer et al. 2005; Lamas et al. 2009; Kraus et al. 2014; Oppermann et al. 2014). Detailed studies of intraosseous vasculatures will be useful for understanding diseases and will help doctors to preserve the blood supplies of bones and therefore, reduce the rates of iatrogenic nonunion and osteonecrosis due to mistaken osteotomy of the nutrient-supplying artery. The vascular supplies of certain areas have been elaborately studied using conventional methods, but iatrogenic avascular osteonecrosis still occurs in clinical practice, and the femoral head serves as a model of this condition. Studies using advanced methods that can illustrate the intraosseous vasculature in an undistorted manner are necessary (Ikemura et al. 2013).

Conventional methods used to investigate intraosseous vasculatures

Injections of dyes into the vascular system have been employed since the 16th century. Latex or epoxy resin has been injected to study the vasculature of the humeral head (Meyer et al. 2005). Corrosion casts can be prepared by dissolving the soft tissues (Schiltenwolf et al. 1996). Some researchers have been able to display intraosseous vasculatures by injecting specimens with latex, epoxy resin or radiocontrast agents or by making serial bone sections to reconstruct the arteries (Lamas et al. 2009). The above-mentioned methods all have notable disadvantages. The injection of non-radiocontrast agents requires the subsequent application of the Spalteholz transparency technique

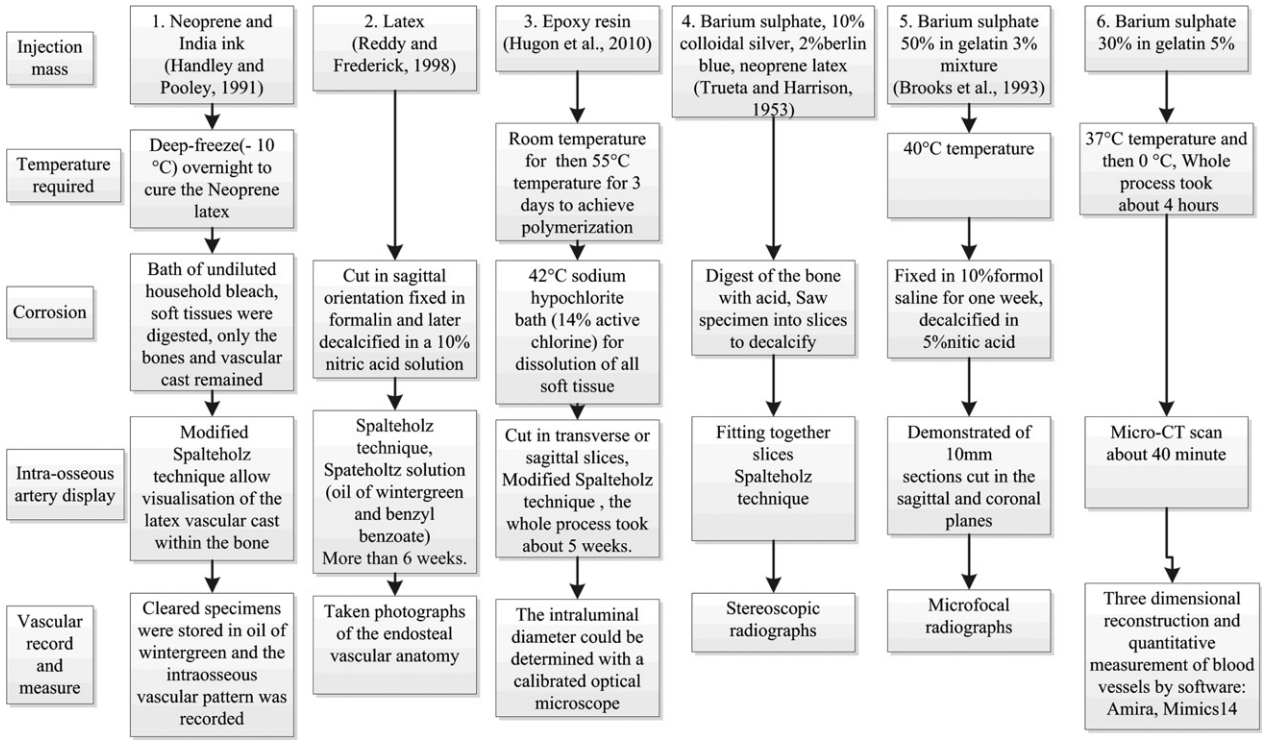

Fig. 4 Comparison of the different technological processes for the perfusion and display of intraosseous blood vessels. Nearly all of the technological processes include injection, corrosion, intraosseous blood vessels display and recording of the vasculature. Technique no. 6 is the simplest and requires the least time to produce accurate vascular three-dimensional reconstructions.

by which bone and other tissues are rendered transparent (Lamas et al. 2009). The use of corrosion casts requires the dissolution of the bone, which leads to the loss of some critical information. The Spalteholz transparency technique is time-consuming and complex and begins with decalcification. Decalcification of the femoral head required bone dissection, which inevitably damages the femoral head arterial architecture and undermines the vasculature. Furthermore, using the Spalteholz technique, it is difficult to quantify the vascular diameter and length, and the quantifications of the vessel volume, vessel length density, vessel area density and vessel volume density are almost impossible. Finally, the Spalteholz technique is associated with a high failure rate due to excessive corrosion. The injection of radiocontrast agents followed by plain radiography is only capable of producing two-dimensional images that cannot precisely present the three-dimensional vasculature.

Advantages of micro-CT investigations of the intraosseous vasculature

Recently, micro-computed tomography has emerged as a high-resolution imaging modality that is capable of analysing structures with a pixel size on the order of 10 μm (Campbell & Sophocleous, 2014). Micro-CT, which involves the administration of a contrast agent, has been widely utilized to perform highly accurate quantifications of the three-dimensional vascular networks of tumours, the coronary artery and the entire vasculature of the brain (Lerman & Ritman, 1999; Lee et al. 2007; Langheinrich et al. 2010). Thus far, micro-CT scanning of the intraosseous vasculature following the injection of radiopaque material has only been reported in two papers, both of which claimed that clear and precise results could be obtained (Hananouchi et al. 2010; Zhao et al. 2011). However, the imaging techniques and overall imaging quality could still be improved.

To our best knowledge, this is the first study to visualize and quantify normal human femoral head intraosseous arteries using micro-CT. The present study demonstrated the site where the nutrition-carrying artery enters the bone and the intraosseous artery trunk and branches. The arterioles and intraosseous arterial anastomoses were all clearly demonstrated. Barium sulphate does not pass into the veins but fills the arteries, arterioles, sinusoids and perhaps the large capillaries, whereas the capillary anastomoses are not demonstrated (Sevitt & Thompson, 1965).

In addition to the excellent presentation of the morphology, this technique allows for the quantification of various aspects of the blood vessels, including the artery diameter, length, and volume and the artery length and volume densities, using software programs (Lerman & Ritman, 1999; Ehling et al. 2014). Furthermore, the entire process requires only 1 day. This technique can serve as an effective research

tool for studying the mechanisms underlying bone diseases, such as bone necrosis, osteoporosis, bone flap transplantation and other metabolic conditions of the bone associated with osseous blood supply disruptions or abnormalities.

The barium sulphate suspension used in this study

Contrast agents composed of barium sulphate can enter the arterioles but are virtually incapable of entering the veins through the capillaries (Sevitt & Thompson, 1965). The atomic weight of barium is several fold greater than that of calcium, which is the main component of bone. This property endows barium sulphate with a greater Hounsfield unit value, which enabled the clear demonstration of the contrast-filled intraosseous artery without the need for bone decalcification. A 30% barium sulphate solution is an appropriate concentration for obtaining high quality images. Barium sulphate is a heavy metal, but it has stable chemical properties and is non-toxic. Barium sulphate is a regular contrast agent that is employed in clinical digestive tract imaging examinations. The injection of barium sulphate suspension into intraosseous arteries can be used for further histological examinations and biomechanical testing.

Limitations

The limitation of this study that should be highlighted is that during *ex vivo* measurement, artefacts due to the shrinkage of the gelatine during hardening occur. Therefore, the measurement results may be smaller than the actual values.

Conclusion

The intravascular perfusion of a barium sulphate suspension combined with micro-CT scanning can produce high-resolution, 3-D digitalized, quantifiable data and images of the entire intraosseous vasculature. This technique does not require bone decalcification or bone dissection. Thus, this technique allows for the easy quantification, preservation and presentation of the intraosseous vasculature and significantly shortens the required experimental time. This method provides a simple and fast technique for quantifying and visualizing human intraosseous vasculature.

Acknowledgements

No funding supplied for this study.

Authors' contributions

Xing Qiu: Literature search, data collection, data analysis, writing. Xiaotian Shi: Literature search, data collection, data analysis. Jun Ouyang: Study design, writing. Dachuan Xu: Study design, data analysis. Dewei Zhao: Literature search, study design, data analysis, data interpretation, writing.

References

Campbell GM, Sophocleous A (2014) Quantitative analysis of bone and soft tissue by micro-computed tomography: applications to ex vivo and in vivo studies. *Bonekey Rep* **3**, 564.

Ehling J, Theek B, Gremse F, et al. (2014) Micro-CT imaging of tumor angiogenesis: quantitative measures describing micromorphology and vascularization. *Am J Pathol* **184**, 431–441.

Hananouchi T, Nishii T, Lee SB, et al. (2010) The vascular network in the femoral head and neck after hip resurfacing. *J Arthroplasty* **25**, 146–151.

Havet E, Duparc F, Tobenas-Dujardin AC, et al. (2008) Vascular anatomical basis of clavicular non-union. *Surg Radiol Anat* **30**, 23–28.

Ikemura S, Hara T, Nakamura T, et al. (2013) Subchondral insufficiency fracture of the femoral head: a report of two cases with a history of internal fixation of a femoral neck fracture. *Skeletal Radiol* **42**, 849–851.

Judet RJ, Lagrange J, Dunoyer J (1955) A study of the arterial vascularization of the femoral neck in adult. *J Bone Joint*, **37-A**, 663–680.

Koslowsky TC, Schliwa S, Koebke J (2011) Presentation of the microscopic vascular architecture of the radial head using a sequential plastination technique. *Clin Anat* **24**, 721–732.

Kraus JC, McKeon KE, Johnson JE, et al. (2014) Intraosseous and extraosseous blood supply to the medial cuneiform: implications for dorsal opening wedge plantarflexion osteotomy. *Foot Ankle Int* **35**, 394–400.

Lamas C, Llusa M, Mendez A, et al. (2009) Intraosseous vascularity of the distal radius: anatomy and clinical implications in distal radius fractures. *Hand (NY)* **4**, 418–423.

Langheinrich AC, Yeniguen M, Ostendorf A, et al. (2010) Evaluation of the middle cerebral artery occlusion techniques in the rat by in-vitro 3-dimensional micro- and nano computed tomography. *BMC Neurol* **10**, 36.

Lee J, Beighley P, Ritman E, et al. (2007) Automatic segmentation of 3D micro-CT coronary vascular images. *Med Image Anal* **11**, 630–647.

Lerman A, Ritman EL (1999) Evaluation of microvascular anatomy by micro-CT. *Herz* **24**, 531–533.

McKeon KE, McCormick JJ, Johnson JE, et al. (2012) Intraosseous and extraosseous arterial anatomy of the adult navicular. *Foot Ankle Int* **33**, 857–861.

Meyer C, Alt V, Hassanin H, et al. (2005) The arteries of the humeral head and their relevance in fracture treatment. *Surg Radiol Anat* **27**, 232–237.

Oppermann J, Franzen J, Spies C, et al. (2014) The microvascular anatomy of the talus: a plastination study on the influence of total ankle replacement. *Surg Radiol Anat* **36**, 487–494.

Papakonstantinou MK, Pan WR, le Roux CM, et al. (2012) New approach to the study of intraosseous vasculature. *ANZ J Surg* **82**, 704–707.

Schiltenwolf M, Martini AK, Mau HC, et al. (1996) Further investigations of the intraosseous pressure characteristics in necrotic lunates (Kienbock's disease). *J Hand Surg Am* **21**, 754–758.

Sevitt S, Thompson RG (1965) The distribution and anastomoses of arteries supplying the head and neck of the femur. *J Bone Joint Surg Br* **47**, 560–573.

Sheetz KK, Bishop AT, Berger RA (1995) The arterial blood supply of the distal radius and ulna and its potential use in vascularized pedicled bone grafts. *J Hand Surg Am* **20**, 902–914.

Trueta J, Harrison M (1953) *The normal vascular anatomy of the femoral head in adult man*, Ludgate House.

Zhao B, Fan M, Wang AY (2011) Quantification and 3-D reconstruction of bone and intraosseous vessels. *Orthoped J China* **19**, 2072–2076.

Supporting Information

Additional Supporting Information may be found in the online version of this article:

Video S1. 3-D reconstruction of the left femoral head and the intraosseous arterial net. The superior retinacular artery (SRA), the inferior retinacular artery (IRA) and the anterior retinacular artery (ARA) anastomoses within femoral head. The epiphyseal plate is an anatomical landmark of the the epiphyseal basilar artery network. Three-dimensional orthogonal projection views of the intraosseous arterial network of the left femoral head: Coronal view (video S1), medial-sagittal view (video S2).

Video S2. Three-dimensional orthogonal projection views of the intraosseous arterial network of the left femoral head. Coronal view (A), medial-sagittal view (B), transverse view (C), and 3-D orthogonal projection (D) views of the left femoral head showing the anastomoses of the superior (SRA), inferior (IRA) and anterior (ARA) retinacular arteries. M, L, A and P corresponds to medial, lateral, anterior and posterior, respectively.